OLYMPUS: First measurement of the charge-averaged elastic lepton-proton cross section

J. C. Bernauer,[1,2,*] A. Schmidt,[3,4,†] B. S. Henderson,[4] L.D. Ice,[5] D. Khaneft,[6] C. O'Connor,[4] R. Russell,[4] N. Akopov,[7] R. Alarcon,[5] O. Ates,[8] A. Avetisyan,[7] R. Beck,[9] S. Belostotski,[10,‡] J. Bessuille,[4] F. Brinker,[11] J. R. Calarco,[12] V. Carassiti,[13] E. Cisbani,[14] G. Ciullo,[13] M. Contalbrigo,[13] R. De Leo,[15] J. Diefenbach,[8] T. W. Donnelly,[4] K. Dow,[4] G. Elbakian,[7] P. D. Eversheim,[9] S. Frullani,[14,‡] Ch. Funke,[9] G. Gavrilov,[10] B. Gläser,[6] N. Görrissen,[11] D. K. Hasell,[4] J. Hauschildt,[11] Ph. Hoffmeister,[9] Y. Holler,[11] E. Ihloff,[4] A. Izotov,[10] R. Kaiser,[16] G. Karyan,[11,7] J. Kelsey,[4] A. Kiselev,[10] P. Klassen,[9] A. Krivshich,[10] M. Kohl,[8,§] I. Lehmann,[16] P. Lenisa,[13] D. Lenz,[11] S. Lumsden,[16] Y. Ma,[6] F. Maas,[6] H. Marukyan,[7] O. Miklukho,[10] R. G. Milner,[4] A. Movsisyan,[7,13] M. Murray,[16] Y. Naryshkin,[10] R. Perez Benito,[6] R. Perrino,[15] R. P. Redwine,[4] D. Rodríguez Piñeiro,[6] G. Rosner,[16] U. Schneekloth,[11] B. Seitz,[16] M. Statera,[13] A. Thiel,[9] H. Vardanyan,[7] D. Veretennikov,[10] C. Vidal,[4] A. Winnebeck,[4] and V. Yeganov[7]

(The OLYMPUS Collaboration)

[1] *Stony Brook University, Stony Brook, NY, 11794, USA*
[2] *Riken BNL Research Center, Upton, NY, 11793, USA*
[3] *George Washington University, Washington, DC, 20052, USA*
[4] *Massachusetts Institute of Technology, Cambridge, MA 02139, USA*
[5] *Arizona State University, Tempe, AZ 85281, USA*
[6] *Johannes Gutenberg-Universität, Mainz, Germany*
[7] *Alikhanyan National Science Laboratory (Yerevan Physics Institute), Yerevan, Armenia*
[8] *Hampton University, Hampton, VA 23668, USA*
[9] *Rheinische Friedrich-Wilhelms-Universität, Bonn, Germany*
[10] *Petersburg Nuclear Physics Institute, Gatchina, Russia*
[11] *Deutsches Elektronen-Synchrotron, Hamburg, Germany*
[12] *University of New Hampshire, Durham, NH 03824, USA*
[13] *Università degli Studi di Ferrara and Istituto Nazionale di Fisica Nucleare sezione di Ferrara, Ferrara, Italy*
[14] *Istituto Nazionale di Fisica Nucleare sezione di Roma and Istituto Superiore di Sanità, Rome, Italy*
[15] *Istituto Nazionale di Fisica Nucleare sezione di Bari, Bari, Italy*
[16] *University of Glasgow, Glasgow, United Kingdom*

(Dated: July 11, 2020)

We report the first measurement of the average of the electron-proton and positron-proton elastic scattering cross sections. This lepton charge-averaged cross section is insensitive to the leading effects of hard two-photon exchange, giving more robust access to the proton's electromagnetic form factors. The cross section was extracted from data taken by the OLYMPUS experiment at DESY, in which alternating stored electron and positron beams were scattered from a windowless gaseous hydrogen target. Elastic scattering events were identified from the coincident detection of the scattered lepton and recoil proton in a large-acceptance toroidal spectrometer. The luminosity was determined from the rates of Møller, Bhabha and elastic scattering in forward electromagnetic calorimeters. The data provide some selectivity between existing form factor global fits and will provide valuable constraints to future fits.

Precise determination of the proton form factors is critical for the understanding of the proton internal dynamics, giving direct access to the distribution of charge and magnetization in the nucleus. They are touchstones for the verification of theoretical descriptions and computational approaches. For large Q^2, the progress in precision measurements are hampered by the unresolved discrepancy between measurements of the proton's elastic form factor ratio, $\mu_p G_E^p/G_M^p$, using polarization techniques [1–8], and those obtained using the traditional Rosenbluth technique in unpolarized cross section measurements [9–14].

One hypothesis for the cause of this discrepancy is a contribution to the cross section from hard two-photon exchange (TPE), which is not included in standard radiative corrections and would affect the two measurement techniques differently [15–20].

Standard radiative correction prescriptions account for two-photon exchange only in the soft limit, in which one photon carries negligible momentum [21, 22]. There is no model-independent formalism for calculating hard TPE. Some model-dependent calculations suggest that TPE is responsible for the form factor discrepancy [17–20] while others contradict that finding [23, 24]. The current status

of the recent experimental and theoretical progress on two-photon exchange is summarized in Ref. [25].

While most models predict negligible effects of hard two-photon exchange on measurements using polarization, such measurements can only extract the form factor ratio. A separation of G_E and G_M requires absolute measurements of the lepton-proton cross section, which are affected by hard TPE. To leading order, TPE effects depend on the charge-sign of the lepton. Therefore, a charge-averaged cross section is far less sensitive to TPE. We report here on the first precision determination of a charge-averaged cross section of $e^{\pm} - p$ scattering.

OLYMPUS's main goal was to measure the ratio of the cross sections for positron-proton and electron-proton scattering, a quantity which gives direct access to the two-photon exchange correction. OLYMPUS was optimized for this purpose, and the results are published in Ref. [26]. However, careful further analysis allowed us to extract charge-averaged cross sections. They cover an interesting kinematical region, where existing form factor fits show a turn-over behavior for G_M, and where the existing data for $e^- p$ scattering is somewhat lacking, leading to large model uncertainties.

Only a brief overview of the OLYMPUS experiment is given here, and we refer to [27] for a detailed description of the detector. OLYMPUS was the last experiment to take data at the DORIS electron/positron storage ring at DESY, Hamburg, Germany. In total, an integrated luminosity of 4.5 fb^{-1} was collected. The 2.01 GeV stored beams with up to 65 mA of current passed through an internal, unpolarized hydrogen gas target with an areal density of approximately 3×10^{15} atoms/cm^2 [28]. The accelerator magnet power supplies were modified to allow the daily change of beam species.

The main detector, a toroidal magnetic spectrometer, was based on the former MIT-Bates BLAST detector [29], with the two horizontal sections instrumented with large acceptance ($20^\circ < \theta < 80^\circ$, $-15^\circ < \phi < 15^\circ$) drift chambers (DC) for 3D particle tracking and walls of time-of-flight scintillator bars (ToF) for triggering and particle identification. The left-right symmetry of the detector system was used as a cross-check in the analysis. The data presented here were collected entirely with positive-tracks-outbending toroid polarity in order to suppress background rates in the DC, so that low-energy electrons were bent back to the beam axis and away from the detectors.

Two new detector systems were designed and built to monitor the luminosity. These were symmetric Møller/Bhabha calorimeters (SYMB) at 1.29° [30] and two telescopes of three triple gas electron multiplier (GEM) detectors [31] interleaved with three multi-wire proportional chambers (MWPC) mounted at 12°.

The trigger system selected candidate events that resulted from a lepton and proton detected in coincidence in opposite sectors. The data were acquired and stored via the CBELSA/TAPS data acquisition system [32].

The positions of all detector elements were determined via optical surveys and the magnetic field was mapped in-situ throughout the complete tracking volume [33].

Acceptances, radiative corrections and efficiencies were accounted for via a sophisticated Monte Carlo (MC) simulation, which matched the measured time-dependence of the beam current and position, rigorously treating the correlations between effects. The MC simulation used a radiative event generator developed specifically for OLYMPUS [34, 35]. This generator produced lepton-proton events weighted by several different radiative cross section models. In this letter, we present the results following the Maximon-Tjon [22] prescription. Higher order radiative corrections are taken into account through exponentiation.

Particle trajectories and energy losses were simulated using Geant4, with custom digitization routines to produce output identical in format to actual measured data. This step included efficiency and resolution simulations whose parameters were determined from data. Both the simulated and the real data were then analyzed with identical software.

Track reconstruction used a fast hierarchical pattern matching algorithm to identify track candidates. Initial track parameters were then determined via two distinct track fit algorithms.

Particle identification was achieved by a combination of track curvature direction, indicating the particle charge, and the correlation between momentum and time-of-flight to cleanly separate positrons from protons.

The efficiency of the drift chambers was determined by performing track reconstruction without considering one of the drift chamber super-layers and then considering whether or not hits were present in the ignored super-layer. This technique was used to develop highly granular efficiency maps of each drift cell. These maps were used directly in the detector simulation. While the majority of the drift cells had efficiency $> 95\%$, several had reduced efficiency, likely because of high discriminator thresholds. These inefficient cells had only a small effect on the overall tracking efficiency because of the redundancy of the six superlayers.

The efficiency of the time-of-flight scintillators was assessed using the combination of cosmic ray studies, data taken with a prescaled efficiency trigger, and Geant4 simulation. The efficiency was greater than 99% for protons and greater than 97% for electrons. The ToF efficiency model was also implemented in the OLYMPUS simulation.

The track reconstruction efficiency was assessed by selecting elastically recoiling protons in one sector and looking for the corresponding scattered lepton in the other sector. Within the precision of the study, there was no indication of inefficiency beyond that caused by ToF and drift chamber inefficiencies. A normalization

systematic uncertainty of 2% was estimated for any possible difference between the simulated elastic efficiency and that of the experimental data, while a 1% normalization uncertainty was assessed for any possible difference in the track reconstruction performance on simulated versus experimental data.

Four independent elastic event selection routines were developed [34–37], which allowed us to assess the degree of event-selection bias. While the four approaches differ in detail, they all exploit the fact that for a coincidence measurement of elastic scattering the kinematics are over-determined and that selection cuts on the self-consistency of the kinematics can be used to suppress inelastic background. The four analyses found similar levels of background for both lepton species, varying from negligibly small at low Q^2 to $\approx 20\%$ at high Q^2. This background was subtracted and the statistical uncertainty associated with this subtraction was propagated to the final result. Fig. 1 shows an example of the background fit for one of the highest Q^2 bins, where the background contribution was largest.

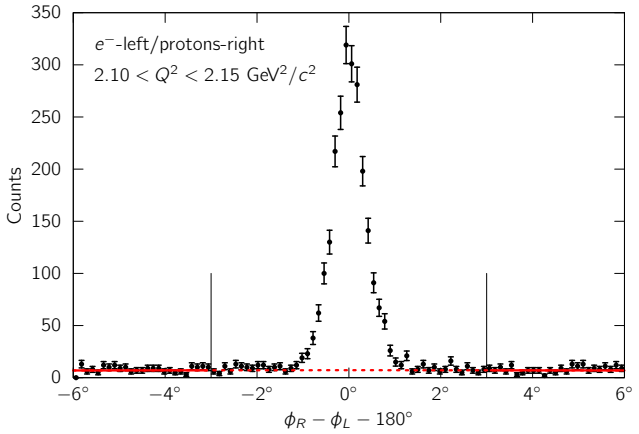

FIG. 1. Background was estimated and subtracted in Ref. [35] using fits to the sidebands of the distribution of the difference in azimuth of lepton (ϕ_L) and proton (ϕ_R) track pairs after all other elastic event selection criteria were applied. The background was largest at high-Q^2, as shown here, with little difference between e^- and e^+ modes.

The total recorded data were screened for optimal running conditions, and a subset corresponding to 3.1 fb^{-1} of integrated luminosity was selected for the results presented here.

OLYMPUS was optimized for a measurement of the cross section ratio between the two beam species, and therefore it employed three independent systems to determine *relative* luminosity: from the elastic rate in the two 12° telescopes, the Møller/BhaBha rate in the SYMB, and from the beam current and target density recorded by the slow control system. For an *absolute* measurement of the luminosity, none of the systems is optimal:

- Fundamentally, the 12° telescopes measure the same process as the main spectrometer and can therefore not give an absolute measurement. It could however extend the Q^2 range of the measurement, so that a different determination of the cross section at this smaller value, (for example, from a fit) would give the normalization and then an quasi-absolute cross section for the remaining data points. However, the 12° telescope acceptance and absolute efficiency is not known well enough to produce a sensible result. The data point is therefore completely omitted here.

- The slow control system could, in principle, give an absolute normalization. However, uncertainties from the target temperature, which affects the density, as well as the absolute calibration of the beam current could not be quantified with a reliable error estimate.

- The most robust SYMB analysis made use of multi-interaction events, in which a symmetric Møller or Bhabha event occurred in the same bunch as an unrelated forward-scattering elastic *ep* event. This method takes advantage of the cancellation of many systematic effects when determining the relative luminosity between beam species. However, these effects do not cancel in the determination of the absolute luminosity, resulting in an uncertainty of 7%.

We note that the results of the SYMB and slow control differ only by about 1%.

We report the average of the cross sections determined by the four independent analyses. We further use the variance between the analyses to estimate some of the systematic uncertainties. To separate point-to-point and normalization uncertainties, we fit normalization constants to the results of each of the four analyses, and minimize the difference to the average. We use the remaining variance to estimate the point-to-point systematic uncertainty from event-selection bias, with the variation between constants used to assess the contribution to the normalization uncertainty (1.5%). The systematic difference between cross sections determined from the lepton-left/proton-right versus proton-right/lepton-left topologies to assess the systematic uncertainty from mis-modeling of the detector acceptance (0.7%). In total, we achieve a global normalization uncertainty of 7.5%, dominated by the luminosity uncertainty. Table I gives an overview.

The OLYMPUS determination of the charge-average cross section, as a function of ϵ and Q^2 is provided in Table II. A comparison of our results with a selection of fits is shown in Fig. 2. The fits presented here use different methods to minimize the influence of TPE on the extracted form factors. All use both Rosenbluth as well as polarized data in their fits, and assume that the influence

TABLE I. Contributions to the systematic uncertainty in the global normalization

Source	Uncertainty in the normalization
Luminosity	7.0%
Efficiency	2.0%
Event Selection	1.5%
Track Reconstruction	1.0%
Detector Acceptance	0.7%
Total	7.5%

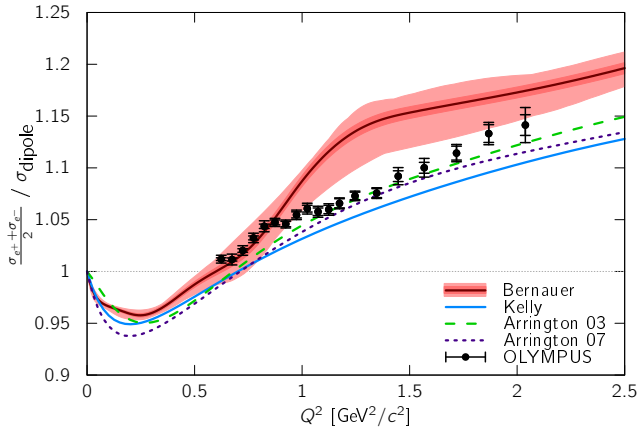

FIG. 2. The data for the charge-average cross section as a function of Q^2, in comparison with a series of predictions from form factor fits [28, 38, 39]. The Bernauer [40] prediction is shown with statistical (inner band) and model dependency systematical error (added linear to statistical error, outer band). As can be deducted from the width of the bands and the difference in the models, the existing data in this range cannot constrain the models very well.

of TPE on the ratio extracted from polarized data is minimal. Kelly [41] omits G_E results for $Q^2 > 1$ (GeV/c)^2 and relies on ratio determinations from polarized experiments and G_M values extracted from e^--p scattering, but does not correct them for hard TPE effects. While the effect of TPE on the extraction is small compared to the effect on G_E at these Q^2, it is not clear *a priori* how large the effect is, and how the uncorrected data at smaller Q^2 affect the high-Q^2 behavior. Arrington 03 [42] uses a phenomenological correction to the cross sections with a linear dependence in ϵ and fixed scale of 6%. Arrington 07 [39] uses theoretical TPE calculations and complements them for data points > 1 (GeV/c)^2 with an ad-hoc additional effect, linear in ϵ and with a scale with logarithmic dependence. Bernauer [28] uses a two-parameter phenomenological model, a combination of the Feshbach correction, valid at $Q^2 = 0$, and a linear model with logarithmic scaling in Q^2, applied to data at all Q^2, fitting form factor parameters and TPE parameters together.

The data presented here connect the well-constrained region below 1 (GeV/c)^2 with the region between 1 and 2 (GeV/c)^2 where TPE effects are more prominent. The fit by Bernauer preferred a strong cusp-like structure in G_M around 1.3 (GeV/c)^2, while the other, less flexible, fits, have a smoother transition. The data seem to be in better agreement with the latter, but a more detailed study of the effects of the new data set on form factor fits must follow.

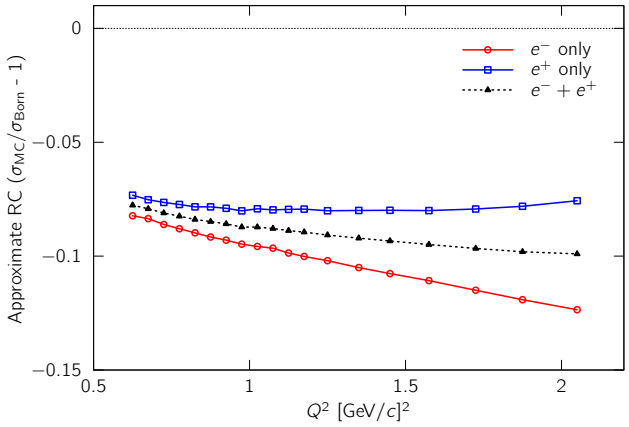

FIG. 3. The approximate radiative correction, estimated by taking the ratio of the simulated cross sections with and without the inclusion of radiative effects. The charge-odd contribution is a sizeable fraction of the total at high Q^2.

The advantage of the charge-averaging technique is illustrated in Fig. 3, which shows the approximate radiative correction for the e^-, e^+, and charge-averaged cross sections, as a function Q^2. These corrections were estimated by comparing the simulated cross sections with and without radiative effects, and so also include the convolution of the effects detector acceptance, efficiency, and resolution. However, the estimates make clear that the charge-odd radiative effects grow to become a sizable fraction of the total at higher Q^2. In forming the charge-average cross section, all of the charge-odd radiative effects are suppressed, not only hard TPE, making the cross section extraction less sensitive to uncertainties in the radiative corrections prescription.

We thank the DORIS machine group and the various DESY groups that made this experiment possible. We gratefully acknowledge the numerous funding agencies: the Ministry of Education and Science of Armenia, the Deutsche Forschungsgemeinschaft, the European Community-Research Infrastructure Activity, the United Kingdom Science and Technology Facilities Council and the Scottish Universities Physics Alliance, the United States Department of Energy and the National Science Foundation, and the Ministry of Education and Science of the Russian Federation. R. Milner also acknowledges the generous support of the Alexander von Humboldt Foundation, Germany.

TABLE II. Cross sections measured by OLYMPUS, using the exponentiated Maximon and Tjon radiative corrections prescription. Uncertainties are statistical and point-to-point systematic. There is a further 7.5% normalization uncertainty that is common to all data points.

$\langle Q^2 \rangle$ [GeV$^2/c^2$]	$\langle \epsilon \rangle$	σ_{e^-p}/std. dipole	σ_{e^+p}/std. dipole	Avg. σ_{ep}/std. dipole
0.624	0.898	$1.0140 \pm 0.0013 \pm 0.0027$	$1.0097 \pm 0.0013 \pm 0.0031$	$1.0119 \pm 0.0013 \pm 0.0035$
0.674	0.887	$1.0155 \pm 0.0015 \pm 0.0032$	$1.0076 \pm 0.0015 \pm 0.0025$	$1.0116 \pm 0.0015 \pm 0.0050$
0.724	0.876	$1.0236 \pm 0.0017 \pm 0.0017$	$1.0169 \pm 0.0016 \pm 0.0033$	$1.0202 \pm 0.0017 \pm 0.0043$
0.774	0.865	$1.0361 \pm 0.0019 \pm 0.0008$	$1.0287 \pm 0.0019 \pm 0.0018$	$1.0324 \pm 0.0019 \pm 0.0042$
0.824	0.853	$1.0475 \pm 0.0022 \pm 0.0035$	$1.0397 \pm 0.0021 \pm 0.0015$	$1.0436 \pm 0.0021 \pm 0.0049$
0.874	0.841	$1.0496 \pm 0.0024 \pm 0.0025$	$1.0451 \pm 0.0023 \pm 0.0016$	$1.0473 \pm 0.0024 \pm 0.0031$
0.924	0.829	$1.0473 \pm 0.0027 \pm 0.0019$	$1.0443 \pm 0.0026 \pm 0.0031$	$1.0458 \pm 0.0026 \pm 0.0028$
0.974	0.816	$1.0545 \pm 0.0030 \pm 0.0030$	$1.0547 \pm 0.0029 \pm 0.0045$	$1.0546 \pm 0.0029 \pm 0.0035$
1.024	0.803	$1.0622 \pm 0.0034 \pm 0.0037$	$1.0591 \pm 0.0032 \pm 0.0044$	$1.0606 \pm 0.0033 \pm 0.0041$
1.074	0.789	$1.0600 \pm 0.0037 \pm 0.0044$	$1.0553 \pm 0.0035 \pm 0.0011$	$1.0576 \pm 0.0036 \pm 0.0039$
1.124	0.775	$1.0619 \pm 0.0041 \pm 0.0031$	$1.0577 \pm 0.0039 \pm 0.0034$	$1.0598 \pm 0.0040 \pm 0.0038$
1.174	0.761	$1.0653 \pm 0.0045 \pm 0.0026$	$1.0663 \pm 0.0043 \pm 0.0035$	$1.0658 \pm 0.0044 \pm 0.0029$
1.246	0.739	$1.0729 \pm 0.0037 \pm 0.0028$	$1.0730 \pm 0.0035 \pm 0.0034$	$1.0729 \pm 0.0036 \pm 0.0029$
1.347	0.708	$1.0769 \pm 0.0045 \pm 0.0033$	$1.0743 \pm 0.0042 \pm 0.0016$	$1.0756 \pm 0.0043 \pm 0.0028$
1.447	0.676	$1.0976 \pm 0.0054 \pm 0.0016$	$1.0864 \pm 0.0050 \pm 0.0032$	$1.0920 \pm 0.0052 \pm 0.0064$
1.568	0.635	$1.0944 \pm 0.0055 \pm 0.0035$	$1.1058 \pm 0.0050 \pm 0.0052$	$1.1001 \pm 0.0053 \pm 0.0073$
1.718	0.581	$1.1125 \pm 0.0070 \pm 0.0064$	$1.1160 \pm 0.0065 \pm 0.0027$	$1.1142 \pm 0.0067 \pm 0.0049$
1.868	0.524	$1.1325 \pm 0.0089 \pm 0.0098$	$1.1338 \pm 0.0083 \pm 0.0018$	$1.1331 \pm 0.0086 \pm 0.0066$
2.038	0.456	$1.1326 \pm 0.0103 \pm 0.0084$	$1.1500 \pm 0.0097 \pm 0.0128$	$1.1413 \pm 0.0100 \pm 0.0137$

* jan.bernauer@stonybrook.edu
† axelschmidt@gwu.edu
‡ deceased

§ partially supported by Jefferson Lab

[1] B. Hu *et al.*, Polarization transfer in the ^{2}H($\vec{e}, e'\vec{p}$)n reaction up to $Q^2 = 1.61$˜(GeV/c)^2, Phys. Rev. **C73**, 064004 (2006).

[2] G. MacLachlan *et al.*, The ratio of proton electromagnetic form factors via recoil polarimetry at $Q^2 = 1.13$˜(GeV/c)^2, Nucl. Phys. **A764**, 261 (2006).

[3] O. Gayou *et al.*, Measurements of the Elastic Electromagnetic Form Factor Ratio $\mu_p G_{E_p}/G_{M_p}$ via Polarization Transfer, Phys. Rev. **C64**, 038202 (2001).

[4] V. Punjabi *et al.*, Proton elastic form factor ratios to $Q^2 = 3.5$˜GeV^2 by polarization transfer, Phys. Rev. **C71**, 055202 (2005).

[5] M. K. Jones *et al.*, Proton G_E/G_M from beam-target asymmetry, Phys. Rev. **C74**, 035201 (2006).

[6] A. J. R. Puckett *et al.*, Recoil Polarization Measurements of the Proton Electromagnetic Form Factor Ratio to $Q^2 = 8.5$˜GeV^2, Phys. Rev. Lett. **104**, 242301 (2010).

[7] M. Paolone *et al.*, Polarization Transfer in the ^{4}He($\vec{e}, e'\vec{p}$)^{3}H Reaction at $Q^2 = 0.8$ and 1.3˜(GeV/c)^2, Phys. Rev. Lett. **105**, 072001 (2010).

[8] A. J. R. Puckett *et al.*, Final analysis of proton form factor ratio data at $Q^2 = 4.0$, 4.8, and 5.6 GeV^2, Phys. Rev. **85**, 045203 (2012).

[9] J. Litt *et al.*, Measurement of the ratio of the proton form-factors, G_E/G_M, at high momentum transfers and the question of scaling, Phys. Lett. **B31**, 40 (1970).

[10] W. Bartel *et al.*, Measurement of proton and neutron electromagnetic form factors at squared four-momentum transfers up to 3˜(GeV/c)^2, Nucl. Phys. **B58**, 429 (1973).

[11] L. Andivahis *et al.*, Measurements of the electric and magnetic form factors of the proton from $Q^2 = 1.75$ to 8.83˜(GeV/c)^2, Phys. Rev. **D50**, 5491 (1994).

[12] R. C. Walker *et al.*, Measurements of the proton elastic form factors for $1 \leq Q^2 \leq 3$ (GeV/c)^2 at SLAC, Phys. Rev. **D49**, 5671 (1994).

[13] M. E. Christy *et al.*, Measurements of electron-proton elastic cross sections for $0.4 < Q^2 < 5.5$˜(GeV/c)^2, Phys. Rev. **C70**, 015206 (2004).

[14] I. A. Qattan *et al.*, Precision Rosenbluth measurement of the proton elastic form factors, Phys. Rev. Lett. **94**, 142301 (2005).

[15] P. A. M. Guichon and M. Vanderhaeghen, How to Reconcile the Rosenbluth and the Polarization Transfer Method in the Measurement of the Proton Form Factors, Phys. Rev. Lett. **91**, 142303 (2003).

[16] P. G. Blunden, W. Melnitchouk, and J. A. Tjon, Two photon exchange and elastic electron proton scattering, Phys. Rev. Lett. **91**, 142304 (2003).

[17] Y. C. Chen *et al.*, Partonic Calculation of the Two-Photon Exchange Contribution to Elastic Electron-Proton Scattering at Large Momentum Transfer, Phys. Rev. Lett. **93**, 122301 (2004).

[18] A. V. Afanasev *et al.*, The Two-photon exchange contribution to elastic electron-nucleon scattering at large momentum transfer, Phys. Rev. **D72**, 013008 (2005).

[19] P. G. Blunden, W. Melnitchouk, and J. A. Tjon, Two-photon exchange in elastic electron-nucleon scattering, Phys. Rev. **C72**, 034612 (2005).

[20] S. Kondratyuk, P. G. Blunden, W. Melnitchouk, and

J. A. Tjon, Δ Resonance Contribution to Two-Photon Exchange in Electron-Proton Scattering, Phys. Rev. Lett. **95**, 172503 (2005).

[21] L. W. Mo and Y.-S. Tsai, Radiative Corrections to Elastic and Inelastic e p and mu p Scattering, Rev. Mod. Phys. **41**, 205 (1969).

[22] L. C. Maximon and J. A. Tjon, Radiative corrections to electron proton scattering, Phys. Rev. **C62**, 054320 (2000).

[23] Yu. M. Bystritskiy, E. A. Kuraev, and E. Tomasi-Gustafsson, Structure function method applied to polarized and unpolarized electron-proton scattering: A solution of the GE(p)/GM(p) discrepancy, Phys. Rev. **C75**, 015207 (2007).

[24] E. A. Kuraev, V. V. Bytev, S. Bakmaev, and E. Tomasi-Gustafsson, Charge asymmetry for electron (positron)-proton elastic scattering at large angle, Phys. Rev. **C78**, 015205 (2008), arXiv:0710.3699 [hep-ph].

[25] A. Afanasev *et al.*, Two-photon exchange in elastic electron–proton scattering, Prog. Part. Nucl. Phys. **95**, 245 (2017).

[26] B. S. Henderson *et al.* (OLYMPUS), Hard Two-Photon Contribution to Elastic Lepton-Proton Scattering: Determined by the OLYMPUS Experiment, Phys. Rev. Lett. **118**, 092501 (2017), arXiv:1611.04685 [nucl-ex].

[27] R. Milner, D. K. Hasell, M. Kohl, U. Schneekloth, *et al.*, The OLYMPUS Experiment, Nucl. Instr. Meth. **A741**, 1 (2014).

[28] J. C. Bernauer *et al.*, The OLYMPUS Internal Hydrogen Target, Nucl. Instr. Meth. **A755**, 20 (2014).

[29] D. K. Hasell *et al.*, The BLAST experiment, Nucl. Instr. Meth. **A603**, 247 (2009).

[30] R. Perez Benito *et al.*, Design and Performance of a Lead Fluoride Detector as a Luminosity Monitor, Nucl. Instr. Meth. **A826**, 6 (2016).

[31] O. Ates, Ph.D. thesis, Hampton University, Hampton, Virginia (2014).

[32] A. Thiel *et al.*, Well-established nucleon resonances revisited by double-polarization measurements, Phys. Rev. Lett. **109**, 102001 (2012), arXiv:1207.2686 [nucl-ex].

[33] J. C. Bernauer *et al.*, Measurement and tricubic interpolation of the magnetic field for the OLYMPUS experiment, Nucl. Instr. Meth. **A823**, 9 (2016).

[34] R. L. Russell, Ph.D. thesis, Massachusetts Institute of Technology, Cambridge, Massachusetts (2016).

[35] A. Schmidt, Ph.D. thesis, Massachusetts Institute of Technology, Cambridge, Massachusetts (2016).

[36] B. S. Henderson, Ph.D. thesis, Massachusetts Institute of Technology, Cambridge, Massachusetts (2016).

[37] J. C. Bernauer, Elastic event selection (2016), unpublished.

[38] J. Arrington, Evidence for two photon exchange contributions in electron proton and positron proton elastic scattering, Phys. Rev. **C69**, 032201 (2004).

[39] J. Arrington, W. Melnitchouk, and J. Tjon, Global analysis of proton elastic form factor data with two-photon exchange corrections, Phys. Rev. C **76**, 035205 (2007), arXiv:0707.1861 [nucl-ex].

[40] J. C. Bernauer *et al.* (A1), Electric and magnetic form factors of the proton, Phys. Rev. **C90**, 015206 (2014).

[41] J. J. Kelly, Simple parametrization of nucleon form factors, Phys. Rev. C **70**, 068202 (2004).

[42] J. Arrington, Implications of the discrepancy between proton form-factor measurements, Phys. Rev. C **69**, 022201 (2004), arXiv:nucl-ex/0309011.